ACS APPLIED MATERIALS & INTERFACES

Research Article

www.acsami.org

Ionic Liquid-Assisted Electropolymerization for Lithographical Perfluorocarbon Deposition and Hydrophobic Patterning

Jhih-Guang Wu,[†,§] Cheng-Yang Lee,[‡,§] Shao-Shuo Wu,[‡] and Shyh-Chyang Luo*[,†]

[†]Department of Materials Science and Engineering, College of Engineering, National Taiwan University, No. 1, Sec. 4, Roosevelt Road, Taipei 10617, Taiwan

[‡]Department of Materials Science and Engineering, National Cheng Kung University, 1 University Road, Tainan 70101, Taiwan

Supporting Information

ABSTRACT: We developed a novel approach for hydrophobic patterning: combining the photolithography technique with ionic-liquid (IL)-based electropolymerization to fabricate a hydrophobic pattern. Perfluoro-functionalized 3,4-ethylenedioxythiophene (EDOT-F) dispersed in ILs was directly electropolymerized on substrates, which were patterned in advance with positive photoresists. The positive photoresists did not dissolve in ionic liquids during the electropolymerization process, and the poly(EDOT-F) film created hydrophobic domains, which resulted in hydrophobic patterning. This approach provides desired patterns with a lateral resolution consistent with the mask for photolithography. Two kinds of modified indium-tin-oxide-coated glass (ITO-glass) substrates were used to demonstrate the feasibility of process for creating a hydrophobic pattern: ITO-glass substrates coated with nanostructured PEDOT, and the same substrates coated with Au nanoparticles. By confining water droplets on these two patterned substrates to form droplet arrays, we demonstrated two potential applications: multiple droplet-type electrochemical cells and surface-enhanced Raman scattering platforms. In addition, we also applied this approach to create hydrophobic patterning on ITO-coated polyethylene terephthalate (ITO-PET) substrates. The droplet arrays remained well-organized on the ITO-PET substrates even when the substrates were bent. Our work successfully introduced ILs into the photolithography process, implying great potential for these green solvents.

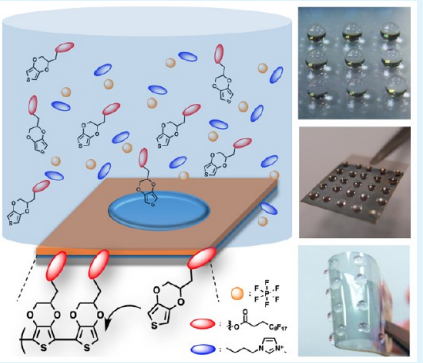

KEYWORDS: *electropolymerization, ionic liquids, lithography, hydrophobic patterning, conducting polymers*

INTRODUCTION

To meet the criteria of real sample screening and high-throughput applications for electroactive films or conducting polymers, the challenge we must overcome is to fabricate films with well-defined microstructures and spatially patterned surface properties. By applying both electropolymerization and functionalized monomers, researchers have demonstrated the feasibility of creating films with control of both surface morphology and the density of surfaces functional groups.[1−5] This technique, combined with patterning methods, creates the opportunities to overcome the aforementioned challenge. Currently, several strategies have been applied in the creation of patterned conducting polymers (CPs) by direct electropolymerization. The bipolar electrochemical method presents the possibility of directly creating gradient surfaces and microsize pattering during electropolymerization.[6−8] By applying anodic aluminum oxide or polystyrene beads as hard templates, researchers have formed nanostructured CP arrays directly on conductive substrates.[9,10] The overoxidation method has been used to selectively insulate certain areas of CPs and create patterns.[11] Although certain successes have been achieved, most of these methods are rather sophisticated and cannot, without difficulty, produce patterns in large scales. A simple fabrication method with high productivity is needed for this purpose.

Because of its simplicity and high efficiency, photolithography is one of the most common techniques used to develop patterns ranging from micro- to submicrosizes on various substrates.[12] This technique has been routinely used in the electronic and semiconducting industries for fabricating integrated circuits. On the basis of the chemistry of photoresist materials, two types of photoresists are applied for lithography processes. A negative photoresist cross-links during the exposure to light, thereby preventing the removal by developing solutions. A typical example of a negative photoresist is Su-8, which has excellent mechanical and chemical stability.[13] Currently, it is extensively used as a master board for fabricating polydimethylsiloxane microfluidic channels.[14] In contract, a positive photoresist degrades after exposure to light and can be removed with developing solutions due to the increased solubility. After the pattern is transferred, the positive photoresist can be totally removed with an organic solvent wash, such as an acetone wash. Although photolithography is a

Received: June 22, 2016
Accepted: August 10, 2016

DOI: 10.1021/acsami.6b07578
ACS Appl. Mater. Interfaces XXXX, XXX, XXX−XXX

Scheme 1. Schematic Illustration Showing the Fabrication of the Hydrophobic Patterns on PEDOT-Coated and AuNP-Coated ITO Substrates[a]

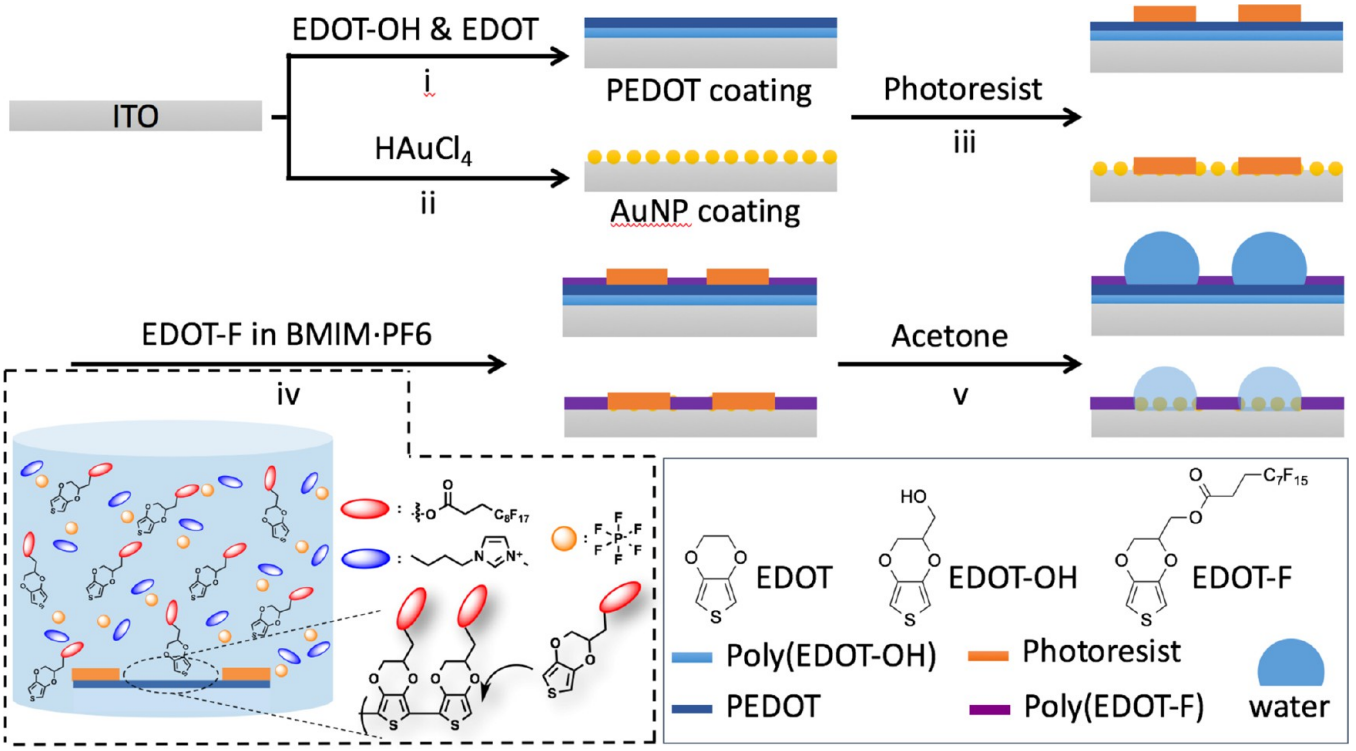

[a](i) Electropolymerization of PEDOT and poly(EDOT-OH); (ii) electrodeposition of AuNP; (iii) photolithography creating patterns via positive photoresist; (iv) electropolymerization of poly(EDOT-F) in ILs; (v) photoresist removal via an acetone wash.

simple technique, the combination of this technique with electropolymerization or electrodeposition to create patterned thin films has proven challenging. The main issue is that the photoresist can easily dissolve in organic solvents, a fact that prohibits the use of organic electrolytes and solvents during electrodeposition or electropolymerization. Thus far, either the electropolymerization and photolithography must take place in aqueous solutions,[15−17] or an uncommon silane-based polymer must be used as a positive photoresist for electrochemical deposition in an acetonitrile solution.[18,19] However, these results do not carry over to most organic compounds, which can dissolve only in dichloromethane, phenylacetonitrile, or propylene carbonate.

Herein we report a new strategy to address this issue by introducing ionic liquids (ILs) as the electrolytes and solvents during electropolymerization.[20] ILs have been recognized as green solvents due to their high evaporation points. They also provide decent solubility for most compounds and can be used as an alternative for electroplating or electropolymerization in organic solvents.[21−23] Furthermore, ILs usually have high viscosities due to strong electrostatic interaction. Therefore, our idea is to leverage the high viscosities of ILs to create patterns by combining ILs with photolithography techniques. Although ILs also dissolve positive photoresist, the process is rather slow compared to electroplating or electropolymerization. Therefore, the procedure is a kinetically controlled process. We tested the stability of photoresists in ILs (Figure S1). The positive photoresist did not dissolve in ILs within a short time (<10 min). On this time scale, the application of electrical stimuli on the substrates did not influence the test results.

In this work, we provided proof of concept by directly electropolymerizing perfluoro-functionalized 3,4-ethylenedioxythiophene (EDOT-F) on photoresist-patterned substrates in an IL, 1-ethyl-3-methyl-imidazolium hexafluorophosphate (EMIM·PF_6) solution as shown in Scheme 1. The perfluorocarbon has been widely used to create hydrophobic or superhydrophobic surfaces depending on their morphologies and surface structures.[24−26] Several researchers have also demonstrated the feasibility of superhydrophobic CPs for tailoring of fluorocarbon on the surface of polymer films.[27−30] By combining the electrodeposition of perfluorocarbon with photolithography techniques, we were able to create a well-defined hydrophobic pattern, which can be used to confine the water droplets on substrates. To demonstrate the feasibility of this process, we used two kinds of modified indium-tin-oxide-coated glass (ITO-glass) substrates: ITO-glass modified with nanostructured PEDOT, and ITO-glass modified with Au nanoparticles (AuNPs). The nanostructured PEDOT and AuNPs could be directly deposited on an ITO surface through electropolymerization and electrodeposition, respectively. After a standard photolithography process, both substrates with patterned positive photoresists were immersed into ILs containing EDOT-F monomers for the deposition of hydrophobic polymer layers. Lastly, the positive photoresists were removed with an acetone wash, and conductive substrates with well-organized hydrophobic patterns were fabricated.

EXPERIMENTAL METHODS

Chemicals and Materials. All chemicals were from commercial sources and used without purification. Both 3,4-ethylenedioxythiophene (EDOT) and hydroxymethyl EDOT (EDOT-OH) were

DOI: 10.1021/acsami.6b07578
ACS Appl. Mater. Interfaces XXXX, XXX, XXX−XXX

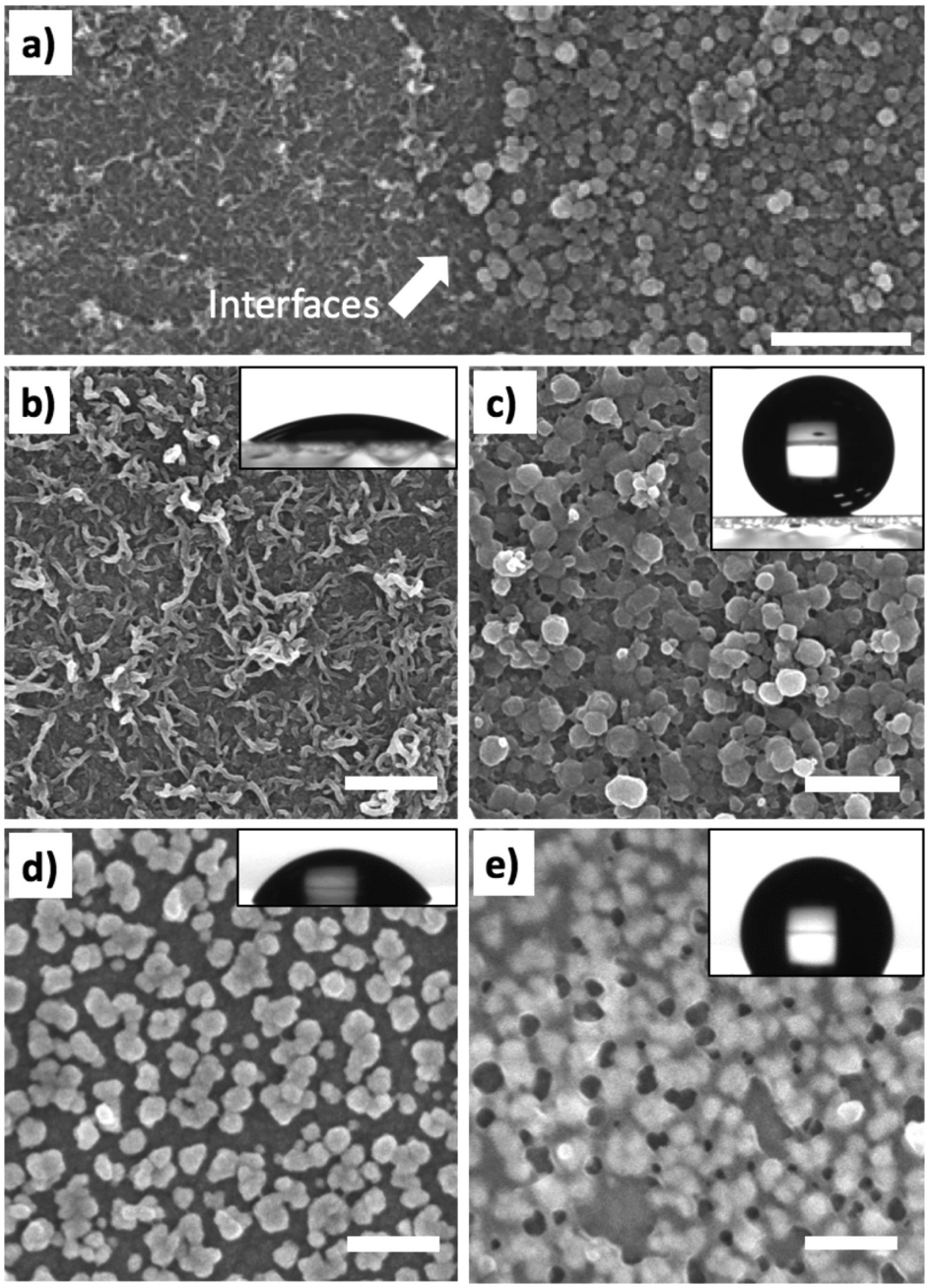

Figure 1. SEM showing the surface morphology of (a) the interface between hydrophilic (PEDOT) and hydrophobic (poly(EDOT-F)) parts; (b) fibrous nanostructure of PEDOT compared to (c) granular nanostructures after addition of the poly(EDOT-F) coating; (d) AuNP surface compared to (e) after addition of the poly(EDOT-F) coating. Contact angle results indicate a hydrophobic surface after addition of the poly(EDOT-F) coating. The scale bar represents 1 μm for part a and 500 nm for parts b–e.

purchased from Sigma-Aldrich. ITO-PET (indium-tin-oxide-coated polyethylene terephthalate film, 60 Ω/sq) was purchased from Uni-Onward Inc. All chemicals for the synthesis of EDOT-F were purchased from Sigma-Aldrich. EDOT-F was synthesized by following a previous report.[9,31] In short, 2*H*,2*H*,3*H*,3*H*-perfluoroundecanoic acid (492.2 mg, 1.00 mmol) was first activated by *N*,*N*′-dicyclohexylcarbodiimide (DCC, 216.7 mg, 1.06 mmol) and 4-dimethylamino pyridine (DMAP, 14.0 mg, 0.11 mmol) in dichloromethane (15.0 mL). The mixture was stirred gently for 1 h under N_2 at room temperature. Afterward, EDOT-OH (190 mg, 1.10 mmol) was added into the solution. The solution was continuously stirred for 16 h before HCl aqueous solution (1 N, 100 mL) was poured into the solution to stop the reaction. The mixture was extracted with dichloromethane (100 mL) three times. The combined organic phases were washed with water, dried over $MgSO_4$, and evaporated by rotoevaporation. The crude product was purified by flash chromatography (ethyl acetate/hexane = 1/5) to yield 350 mg of colorless and viscous liquid. The liquid was then transferred to light yellow solid after being kept in a fridge. ^{1}H NMR (400 MHz, $CDCl_3$, δ): 6.38 (d, J = 3.7, 1H), 6.37 (d, J = 3.7, 1H), 4.59 (m, 2H), 4.48 (m, 1H), 4.25 (dd, J = 11.5, 2.0 Hz, 1H), 4.08 (dd, J = 11.5, 6.5 Hz, 1H), 2.71 (t, J = 7.2, 2 H), 2.51 (tt, 2 H, J = 18.6 Hz, J = 7.2 Hz). ^{13}C NMR (100 MHz, $CDCl_3$, δ): 170.8, 141.1, 140.8, 100.2, 100.1, 71.2, 65.4, 63.0, 26.4, 25.3. HRMS (EI) m/z: [M^+] calcd for $C_{18}H_{11}F_{17}O_4S$, 646.0107; found, 646.0109.

Electropolymerization of PEDOT. The electropolymerization was conducted by using a potentiostat (PGSTAT101, Autolab). A Ag/AgCl reference electrode was used for aqueous and ionic liquid solutions. A Ag/Ag^+ reference electrode was used in organic solutions. A Pt wire was used as a counter-electrode. EDOT monomer solution was prepared by dissolving EDOT at a concentration of 10 mM in

DOI: 10.1021/acsami.6b07578
ACS Appl. Mater. Interfaces XXXX, XXX, XXX–XXX

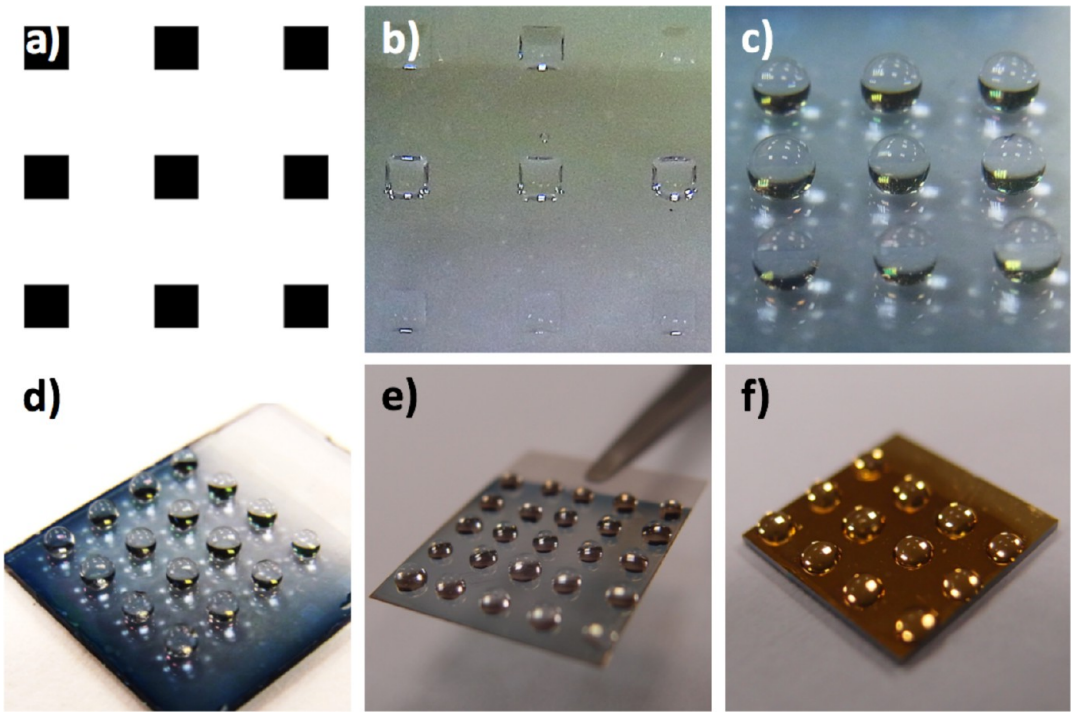

Figure 2. Photo images of (a) photomask with square arrays (1 mm × 1 mm, 2 mm interval), (b) backside of a patterned ITO, and (c) water droplets confined on the hydrophilic part of substrates. The array of water droplets on patterned (d) PEDOT-modified ITO-glass, (e) AuNP-modified ITO-glass, and (f) PEDOT-coated Au substrate.

dichloromethane containing 100 mM tetrabutyl ammonium perchlorate as electrolyte. The solutions were stabilized at 0 °C for 3 min to reach equilibrium before performing electropolymerization. Nanostructured PEDOT was fabricated by electropolymerization using a constant voltage of 1.4 V (vs Ag/Ag^+) for 30 s. EDOT-OH monomer solution was prepared by dissolving EDOT-OH at a concentration of 10 mM in DI water in the presence of 0.1 M $LiClO_4$ and 0.05 M sodium dodecyl sulfate (SDS) as reported previouly.[33] Smooth poly(EDOT-OH) was prepared by applying cyclic potential from −0.6 to 1.1 V (vs Ag/AgCl) at a scan rate of 100 mV/s. Perfluoro-substituent (EDOT-F) solution was prepared by dissolving EDOT-F at a concentration of 20 mM in 1-butyl-3-methylimidazolium hexafluorophosphate, [BMIM][PF_6], ionic liquids. Nanostructured poly(EDOT-F) was prepared by applying two-step constant voltage at 1.4 V (vs Ag/AgCl) for 30 s first, and then at 1.15 V (vs Ag/AgCl) for 180 s.

Electrodeposition of Au Nanoparticles (AuNPs) on ITO. The AuNPs were deposited on ITO substrates directly by applying an electrochemical seed-mediated method.[32] An ITO substrate was first immersed into the solutions containing 0.2 mM $HAuCl_4$ and 0.1 M $NaClO_4$. After that, a constant voltage of −0.8 V (vs Ag/AgCl) was applied for 10 s. Then, the AuNPs were formed by applying a cyclic potential from +0.3 to −0.04 V (vs Ag/AgCl) at scan rate of 50 mV s^{-1} for 300 cycles.

Surface Characterization. The surface morphologies of nanostructured PEDOT and poly(EDOT-F) on ITO and AuNP were examined with field emission scanning electron microscopy (FESEM). FESEM was performed with a Hitachi SU8000 at a vacuum of 10^{-10} Torr under an accelerating voltage of 5 kV. Static contact angle of water (~2 μL) was performed by using a contact angle measurement system (Model 100SB, Sindatek) at room temperature.

Photolithography. The substrates were coated with photoresist (MICROPOSIT S1813) by using a spin coater (Tekstarter Co., Ltd. MSC-300D) at the speed of 4000 rpm for 40 s. Samples were prebaked at 120 °C for 1 min before the exposure. The exposure was conducted by using a single-side mask aligner (OAI 500-IR) with a UV light of 365 nm for 15 s. The development was done by immersing the samples into a developer solution (MICROPOSIT 351 Developer) for 3 min.

Electrochemical Characterization. All electrochemical measurements were performed in a glass cell subjected with an Autolab potentiostat. Ag/AgCl and a Pt electrodes were used as the reference and the counter electrodes, respectively. Cyclic voltammetric measurements were performed in 100 mM $LiClO_4$ aqueous solutions in the presence of 10 mM ferrocyanide over the potential ranging from −0.15 to +0.5 V (vs Ag/AgCl) at scan rates of 10, 25, 50, 100, 250, 500, 1000 mV/s.

SERS Measurement. SERS measurement was performed by using a microscopic Raman system (MRI, Protrustech Co., Ltd., Taiwan). An air-cooling spectrometer (AvaSpec-ULS2048L) of grating 1200 lines/mm and slit 50 μm was used as a detector. An exciting line of 633 nm was supplied by a diode laser (NovaPro) with a power of 75 mW. Portions (3 μL) R6G solutions of various concentration were pipetted on the patterned substrates. After the solutions dried in the air, the measurement was performed with 100% laser power and 30 s integration time.

RESULTS AND DISCUSSION

The surface morphology and water contact angle results are shown in Figure 1. The interface between the hydrophilic and hydrophobic parts was clearly observed, and the transition between these two areas was within a few hundred nanometers (Figure 1a). For the PEDOT-modified ITO, shown in Figure 1b,c, the PEDOT layer of fibrous nanostructures provided a hydrophilic area with low contact angles (28 ± 1.4°). The part with poly(EDOT-F) coating showed granular nanostructures, which provided hydrophobic surfaces with high contact angles (142 ± 5.7°), indicating hydrophobic surfaces. We deposited a poly(EDOT-OH) layer to enhance the adhesion between PEDOT and ITO, which ensured the stability of polymer films during the photolithography process. Without this layer, the PEDOT might peel off during the lithography. For AuNP-modified ITO substrates, the bare AuNPs coating surfaces were

DOI: 10.1021/acsami.6b07578
ACS Appl. Mater. Interfaces XXXX, XXX, XXX−XXX

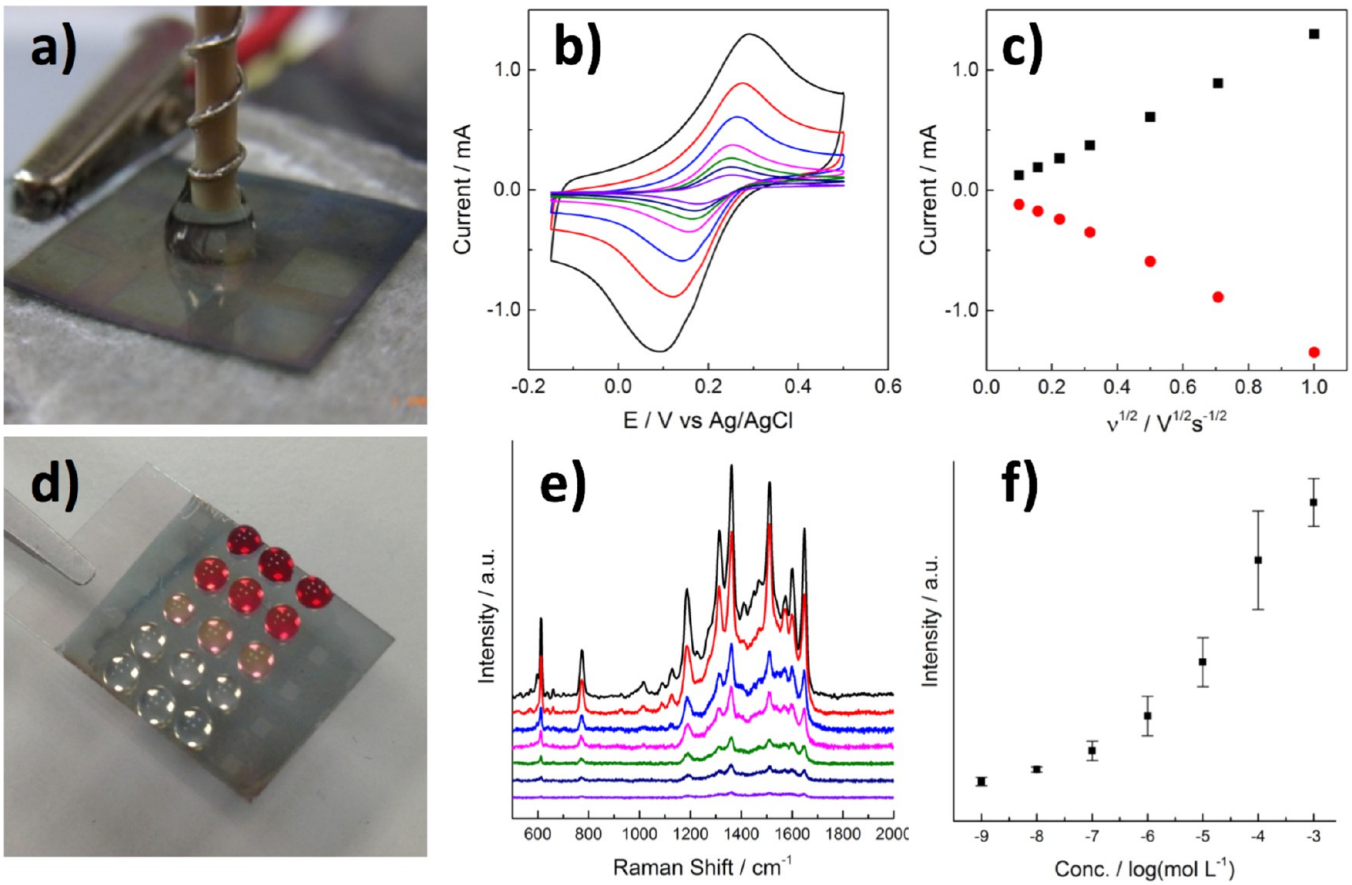

Figure 3. (a) Photo images of droplet-type electrochemical cell setup on a 2 mm × 2 mm pattern. (b) The cyclic voltammogram showing the redox behavior of Fe^{2+}/Fe^{3+} at scan rates of 10 (purple), 20 (navy), 50 (green), 100 (pink), 200 (blue), 500 (red), and 1000 (black) mV s^{-1}. (c) Anodic (black) and cathodic (red) peak current vs square root of scan rate. (d) Photo images of R6G aqueous solutions of 10^{-8}, 10^{-7}, 10^{-6}, 10^{-5}, and 10^{-4} M (left to right). (e) The SERS spectra of R6G of different concentrations (low to high: 10^{-9}, 10^{-8}, 10^{-7}, 10^{-6}, 10^{-5}, 10^{-4}, and 10^{-3} M). (f) The relationship between R6G concentration and intensity of the Raman peak at 1361 cm^{-1}.

hydrophilic, with a contact angle of 63 ± 2.7° (Figure 1d). After the poly(EDOT-F) coating was added, as shown in Figure 1e, the contact angle was increased to 113 ± 3.2°, and the region became hydrophobic.

The design of our initial photomask and the transferred hydrophobic pattern on various ITO-glass substrates as shown in Figure 2. The initial photomask contained square arrays (1 mm × 1 mm), which allowed the transmission of UV light. After the lithography process, the transferred pattern could in most cases be clearly observed from the backside of the ITO-glass substrate (Figure 2b). The water droplets were well-confined by the hydrophobic coating and thus could not spread across the whole surface (Figure 2c). This lithography procedure was successfully applied to PEDOT-modified ITO-glass, AuNP-modified ITO-glass, and Au-coated silica wafer, as, respectively, shown in Figure 2d–f. The water droplets were well-organized and fixed on the patterned substrates. Furthermore, we demonstrated the feasibility to create other shapes of patterns, including circles, diamonds, and rectangles, as shown in Figure S3. By adopting different photomasks, we directly created hydrophobic patterns with different shape and size using the same photolithography process.

The PEDOT-coated ITO-glass and AuNP-coated ITO-glass were used to demonstrate the feasibility of multiple electrochemical and surface-enhanced Raman scattering (SERS) experiments, respectively, as shown in Figure 3. By creating water droplets on conductive substrates, we developed a droplet-type electrochemical cell, as shown in Figure 3a. Due to the size of our reference electrode (2 mm in diameter), we used a 2 mm × 2 mm square pattern for this demonstration. We believe a smaller pattern should also work if a miniaturized reference electrode is used. The counter electrode is a Pt wire wrapped around the Ag/AgCl reference electrode. We observed the redox behavior of Fe^{2+}/Fe^{3+} on PEDOT-coated ITO in the presence of 100 mM $LiClO_4$ as electrolytes by applying cyclic potentials at scan rates of 10, 25, 50, 100, 250, 500, and 1000 mV s^{-1} (Figure 3b). The peak currents were approximately proportional to the square root of the scan rate, as shown in Figure 3c. These peak currents indicated a diffusion-controlled process for this electrochemical setup for our PEDOT-coated ITO platforms. The electrochemical readout was rather consistent, as per our test, and showed less than 5% variation between two spots on the same substrate. We also provide the similar test on an unpatterned PEDOT-coated ITO substrate for comparison, as shown in Figure S4. On the other hand, Rhodamine 6G (R6G) dye was used as the model molecule to demonstrate the multiple SERS measurements on a patterned AuNP-coated substrate, as shown in Figure 3d. The R6G solutions were placed on the AuNP-coated ITO. The Raman spectrum was measured after solutions slowly dried out in an ambient environment; the drying usually took less than 1 h. The SERS spectra of the R6G molecule prepared with different

DOI: 10.1021/acsami.6b07578
ACS Appl. Mater. Interfaces XXXX, XXX, XXX−XXX

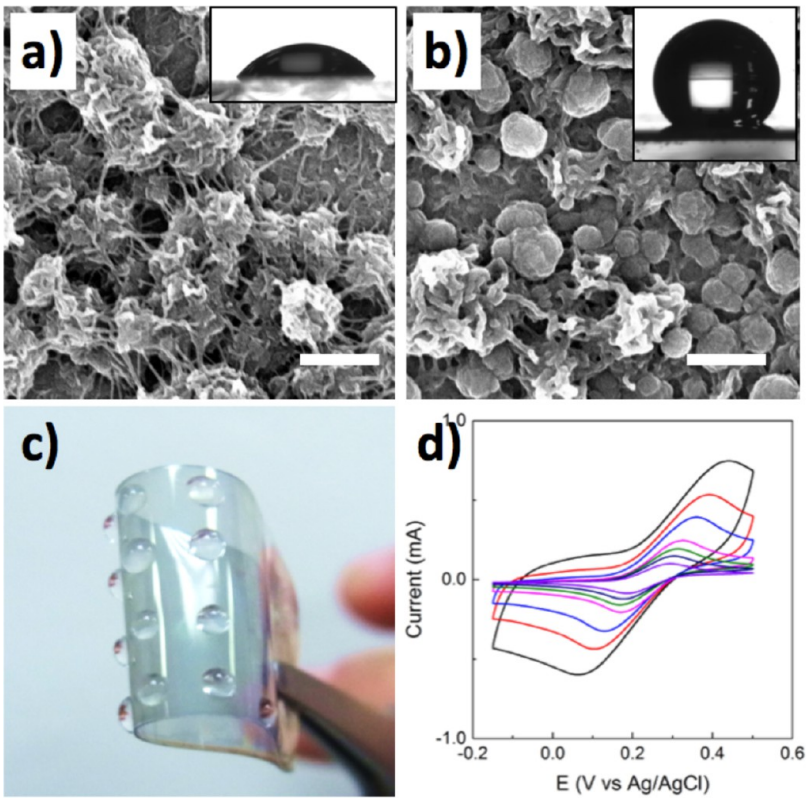

Figure 4. SEM showing the surface morphology of (a) fibrous nanostructure of PEDOT coated on ITO-PET substrates compared to (b) granular nanostructures after the addition of the poly(EDOT-F) coating on PEDOT. Water contact angle results indicating hydrophobic surface after the addition of the poly(EDOT-F) coating. The scale bar represents 500 nm. (c) Photo images of PEDOT-coated ITO-PET film. (d) The cyclic voltammogram showing the redox behavior of Fe^{2+}/Fe^{3+} at scan rates of 10 (purple), 20 (navy), 50 (green), 100 (pink), 200 (blue), 500 (red), and 1000 (black) mV s^{-1}.

solution concentrations (10^{-9}, 10^{-8}, 10^{-7}, 10^{-6}, 10^{-5}, 10^{-4}, and 10^{-3} M) are shown in Figure 3e. We evaluated the relationships between the concentration and SERS activity by monitoring the intensity of the Raman peak at 1361 cm^{-1} as shown in Figure 3f. The deviation was higher than that of the electrochemical readout, mainly due to the inhomogeneous adsorption of R6G molecules on AuNPs. By applying multiple tests on the same chip, we estimated the deviation, observing a satisfactory intensity−concentration trend.

We also tested this process on ITO-coated polyethylene terephthalate (ITO-PET) substrates, as shown in Figure 4. As with the case of nanostructured PEDOT deposited on ITO-glass, we also observed fibrous nanostructures from PEDOT as shown in Figure 4a. The PEDOT morphology on ITO-PET was not as homogeneous as on ITO-glass, which is mainly due to different ITO quality on PET compared to that on glass substrates. During the electropolymerization of PEDOT, the oxidation potential was higher on ITO-PET than on ITO-glass. The low water contact angle (43 ± 5.7°) indicates a hydrophilic surface. On the other hand, poly(EDOT-F) had granular nanostructures and provided hydrophobic surface properties, as shown in Figure 4b. The hydrophobic pattern was also successfully fabricated, and the water droplets remained organized on the patterns when the PET substrates were bent, as shown in Figure 4c. We also examined the electrochemical properties of the patterned ITO-PET substrate by evaluating the Fe^{2+}/Fe^{3+} redox behavior, as shown in Figure 4d. In that figure, it is easy to observe the anodic and cathodic peaks from the cyclic voltammogram. The peaks shifted along with the scanning rate, indicating a diffusion-controlled behavior. The anodic peaks shifted to higher potential on ITO-PET compared to the same test on ITO-glass (Figure 3b), which again was mainly due to the difference in the quality of ITO on PET substrates and on glass substrates. We also noticed that the electrochemical activities decayed on ITO-PET substrates after the substrates were continuously bent.

CONCLUSION

In summary, we successfully demonstrated our new idea of applying ILs to the process of photolithography for pattern transferring. Because the positive photoresist does not quickly dissolve in ILs, the electrodeposition of perfluorocarbon in ILs can be directly electrodeposited on a substrate patterned in advance by photoresists. Substrates of various hydrophobic patterning can be easily fabricated through this process. The array of water droplets can be used for multiple electrochemical or SERS platforms, depending on the substrate properties. Not only did we use the ILs to create hydrophobic patterning, but more importantly, this work provided the first example of using ILs in the photolithography process. Currently, the main concern of this approach is the cost of ILs, which are generally more expensive than other solvents. However, because ILs have high boiling points, the loss due to the evaporation during the process is minimal. In our experiments, we were able to reuse the same IL solutions simply by continuously refilling EDOT-F monomers. Furthermore, ILs are also considered green solvents and environmentally friendly. We expect this approach and

DOI: 10.1021/acsami.6b07578
ACS Appl. Mater. Interfaces XXXX, XXX, XXX−XXX

concept to make a substantial impact on the development of the green industry.

■ ASSOCIATED CONTENT

Supporting Information

The Supporting Information is available free of charge on the ACS Publications website at DOI: 10.1021/acsami.6b07578.

Detailed experimental section, stability test of photoresists in ILs, SEM images, photos of various patterns, and cyclic voltammogram (PDF)

■ AUTHOR INFORMATION

Corresponding Author

*E-mail: shyhchyang@ntu.edu.tw.

Author Contributions

§The manuscript was written through contributions of all authors. All authors have given approval to the final version of the manuscript. J.-G.W. and C.-Y.L contributed equally.

Notes

The authors declare no competing financial interest.

■ ACKNOWLEDGMENTS

We gratefully acknowledge the financial support provided by the Ministry of Science and Technology of Taiwan under Grant MOST 104-2113-M-002-019-MY2 and NSC 102-2113-M-006-013-MY2.

■ ABBREVIATIONS

EDOT, 3,4-ethylenedioxythiophene
CP, conducting polymers
AuNPs, Au nanoparticles
R6G, Rhodamine 6G
SERS, surface-enhanced Raman scattering

■ REFERENCES

(1) Zhu, B.; Luo, S.-C.; Zhao, H.; Lin, H.-A.; Sekine, J.; Nakao, A.; Chen, C.; Yamashita, Y.; Yu, H.-h. Large Enhancement in Neurite Outgrowth on a Cell Membrane-Mimicking Conducting Polymer. *Nat. Commun.* **2014**, *5*, 4523.

(2) Luo, S.-C. Conducting Polymers as Biointerfaces and Biomaterials: A Perspective for a Special Issue of Polymer Reviews. *Polym. Rev.* **2013**, *53*, 303−310.

(3) Chen, C.-H.; Luo, S.-C. Tuning Surface Charge and Morphology for the Efficient Detection of Dopamine under the Interferences of Uric Acid, Ascorbic Acid, and Protein Adsorption. *ACS Appl. Mater. Interfaces* **2015**, *7*, 21931−21938.

(4) Darmanin, T.; de Givenchy, E. T.; Amigoni, S.; Guittard, F. Superhydrophobic Surfaces by Electrochemical Processes. *Adv. Mater.* **2013**, *25*, 1378−1394.

(5) Zhao, H.; Zhu, B.; Sekine, J.; Luo, S.-C.; Yu, H.-h. Oligoethylene-Glycol-Functionalized Polyoxythiophenes for Cell Engineering: Syntheses, Characterizations, and Cell Compatibilities. *ACS Appl. Mater. Interfaces* **2012**, *4*, 680−686.

(6) Inagi, S.; Ishiguro, Y.; Atobe, M.; Fuchigami, T. Bipolar Patterning of Conducting Polymers by Electrochemical Doping and Reaction. *Angew. Chem., Int. Ed.* **2010**, *49*, 10136−10139.

(7) Ishiguro, Y.; Inagi, S.; Fuchigami, T. Site-Controlled Application of Electric Potential on a Conducting Polymer "Canvas". *J. Am. Chem. Soc.* **2012**, *134*, 4034−4036.

(8) Shida, N.; Koizumi, Y.; Nishiyama, H.; Tomita, I.; Inagi, S. Electrochemically Mediated Atom Transfer Radical Polymerization from a Substrate Surface Manipulated by Bipolar Electrolysis: Fabrication of Gradient and Patterned Polymer Brushes. *Angew. Chem., Int. Ed.* **2015**, *54*, 3922−3926.

(9) Lin, H. A.; Luo, S. C.; Zhu, B.; Chen, C.; Yamashita, Y.; Yu, H. H. Molecular or Nanoscale Structures? The Deciding Factor of Surface Properties on Functionalized Poly(3,4-ethylenedioxythiophene) Nanorod Arrays. *Adv. Funct. Mater.* **2013**, *23*, 3212−3219.

(10) Moyen, E.; Hama, A.; Ismailova, E.; Assaud, L.; Malliaras, G.; Hanbuecken, M.; Owens, R. M. Nanostructured Conducting Polymers for Stiffness Controlled Cell Adhesion. *Nanotechnology* **2016**, *27*, 074001.

(11) Isaksson, J.; Kjaell, P.; Nilsson, D.; Robinson, N. D.; Berggren, M.; Richter-Dahlfors, A. Electronic Control of Ca2+ Signalling in Neuronal Cells Using an Organic Electronic Ion Pump. *Nat. Mater.* **2007**, *6*, 673−679.

(12) Gates, B. D.; Xu, Q. B.; Stewart, M.; Ryan, D.; Willson, C. G.; Whitesides, G. M. New Approaches to Nanofabrication: Molding, Printing, and Other Techniques. *Chem. Rev.* **2005**, *105*, 1171−1196.

(13) del Campo, A.; Greiner, C. SU-8: A Photoresist for High-Aspect-Ratio and 3D Submicron Lithography. *J. Micromech. Microeng.* **2007**, *17*, R81−R95.

(14) Jo, B. H.; Van Lerberghe, L. M.; Motsegood, K. M.; Beebe, D. J. Three-Dimensional Micro-Channel Fabrication in Polydimethylsiloxane (PDMS) Elastomer. *J. Microelectromech. Syst.* **2000**, *9*, 76−81.

(15) Gomez, N.; Lee, J. Y.; Nickels, J. D.; Schmidt, C. E. Micropatterned Polypyrrole: A Combination of Electrical and Topographical Characteristics for the Stimulation of Cells. *Adv. Funct. Mater.* **2007**, *17*, 1645−1653.

(16) Kindra, L. R.; Eggers, C. J.; Liu, A. T.; Mendoza, K.; Mendoza, J.; Myers, A. R. K.; Penner, R. M. Lithographically Patterned PEDOT Nanowires for the Detection of Iron(III) with Nanomolar Sensitivity. *Anal. Chem.* **2015**, *87*, 11492−11500.

(17) Jager, E. W. H.; Smela, E.; Inganas, O. Microfabricating Conjugated Polymer Actuators. *Science* **2000**, *290*, 1540−1545.

(18) Schanze, K. S.; Bergstedt, T. S.; Hauser, B. T.; Cavalaheiro, C. S. P. Photolithographically-Patterned Electroactive Films and Electrochemically Modulated Diffraction Gratings. *Langmuir* **2000**, *16*, 795−810.

(19) Schanze, K. S.; Bergstedt, T. S.; Hauser, B. T. Photolithographic Patterning of Electroactive Polymer Films and Electrochemically Modulated Optical Diffraction Gratings. *Adv. Mater.* **1996**, *8*, 531−534.

(20) Plechkova, N. V.; Seddon, K. R. Applications of Ionic Liquids in the Chemical Industry. *Chem. Soc. Rev.* **2008**, *37*, 123−150.

(21) Sekiguchi, K.; Atobe, M.; Fuchigami, T. Electropolymerization of Pyrrole in 1-ethyl-3-methylimidazolium Trifluoromethanesulfonate Room Temperature Ionic Liquid. *Electrochem. Commun.* **2002**, *4*, 881−885.

(22) Liu, Q. X.; El Abedin, S. Z.; Endres, F. Electroplating of Mild Steel by Aluminium in a First Generation Ionic Liquid: A Green Alternative to Commercial Al-Plating in Organic Solvents. *Surf. Coat. Technol.* **2006**, *201*, 1352−1356.

(23) Pringle, J. M.; Efthimiadis, J.; Howlett, P. C.; Efthimiadis, J.; MacFarlane, D. R.; Chaplin, A. B.; Hall, S. B.; Officer, D. L.; Wallace, G. G.; Forsyth, M. Electrochemical Synthesis of Polypyrrole in Ionic Liquids. *Polymer* **2004**, *45*, 1447−1453.

(24) Liu, M.; Jiang, L. Switchable Adhesion on Liquid/Solid Interfaces. *Adv. Funct. Mater.* **2010**, *20*, 3753−3764.

(25) Liu, M.; Wang, S.; Jiang, L. Bioinspired Multiscale Surfaces with Special Wettability. *MRS Bull.* **2013**, *38*, 375−382.

(26) Wang, S.; Liu, K.; Yao, X.; Jiang, L. Bioinspired Surfaces with Superwettability: New Insight on Theory, Design, and Applications. *Chem. Rev.* **2015**, *115*, 8230−8293.

(27) Darmanin, T.; Guittard, F. Molecular Design of Conductive Polymers To Modulate Superoleophobic Properties. *J. Am. Chem. Soc.* **2009**, *131*, 7928−7933.

(28) Darmanin, T.; de Givenchy, E. T.; Amigoni, S.; Guittard, F. Hydrocarbon versus Fluorocarbon in the Electrodeposition of Superhydrophobic Polymer Films. *Langmuir* **2010**, *26*, 17596−17602.

(29) Luo, S.-C.; Liour, S. S.; Yu, H.-h. Perfluoro-Functionalized PEDOT Films with Controlled Morphology as Superhydrophobic

DOI: 10.1021/acsami.6b07578
ACS Appl. Mater. Interfaces XXXX, XXX, XXX−XXX

Coatings and Biointerfaces with Enhanced Cell Adhesion. *Chem. Commun.* **2010**, *46*, 4731−4733.
(30) Darmanin, T.; Guittard, F. Wettability of conducting polymers: From Superhydrophilicity to Superoleophobicity. *Prog. Polym. Sci.* **2014**, *39*, 656−682.
(31) Schwendeman, I.; Gaupp, C. L.; Hancock, J. M.; Groenendaal, L.; Reynolds, J. R. Perfluoroalkanoate-Substituted PEDOT for Electrochromic Device Applications. *Adv. Funct. Mater.* **2003**, *13*, 541−547.
(32) Wang, J.; Cao, X.; Li, L.; Li, T.; Wang, R. Electrochemical Seed-Mediated Growth of Surface-Enhanced Raman Scattering Active Au(111)-Like Nanoparticles on Indium Tin Oxide Electrodes. *J. Phys. Chem. C* **2013**, *117*, 15817−15828.
(33) Luo, S.-C.; Xie, H.; Chen, N.; Yu, H.-h. Trinity DNA Detection Platform by Ultrasmooth and Functionalized PEDOT Biointerfaces. *ACS Appl. Mater. Interfaces* **2009**, *1*, 1414−1419.

DOI: 10.1021/acsami.6b07578
ACS Appl. Mater. Interfaces XXXX, XXX, XXX−XXX